Journal of Applied Polymer Science

Smart composite useful to acid release

Ellen O. Grance,[1] E. R. F. dos Santos,[2] Camila Andrade,[1] G. E. Oliveira,[3] Jose Carlos Pinto,[4] Marcio Nele,[2] Fernando G. Souza Jr.[1,5]

[1]Instituto de Macromoléculas, Centro de Tecnologia - Cidade Universitária, Av. Horácio Macedo, 2030, Bloco J. Universidade Federal de Rio de Janeiro, Brasil

[2]Escola de Química, Centro de Tecnologia - Cidade Universitária, Av. Horácio Macedo, 2030, Bloco E. Universidade Federal de Rio de Janeiro, Brasil

[3]Departamento de Química, Vitória, Av. Fernando Ferrari S/N. Universidade Federal do Espírito Santo, Brasil

[4]Programa de Engenharia Química, COPPE, Centro de Tecnologia - Cidade Universitária, Av. Horácio Macedo, 2030, Bloco G. Universidade Federal de Rio de Janeiro, Brasil

[5]Programa de Engenharia Civil, COPPE, Centro de Tecnologia - Cidade Universitária, Av. Horácio Macedo, 2030, Bloco B. Universidade Federal de Rio de Janeiro, Brasil

Correspondence to: F. G. Souza (E-mail: fgsj@ufrj.br)

ABSTRACT: This work presents a smart composite prepared using a resin based on cardanol and furfural, filled with Al_2O_3. This material is inert at room temperature. However, it is able to release an active substance after a certain temperature is reached. The obtained materials were characterized by Fourier transform spectroscopy, X-ray diffraction, scanning electron microscopy, thermal gravimetric analysis, and differential scanning calorimetry. In addition, cure degree and acid-release tests were performed. According to the obtained data, acid is trapped inside the composites, remaining inactive in the structure while the melting temperature of the hydrophobic shell is not reached. After it is, acid is released and the pH decreases. Therefore, this smart composite could be useful in speeding up drilling in sedimentary rocks with a combination of chemical (acid release) and physical (mechanical wear) mechanisms.
 J. Appl. Polym. Sci. **2016**, *133*, 43071.

KEYWORDS: Biopolymers & renewable polymers; composites; oil & gas

Received 12 August 2015; accepted 18 October 2015
DOI: 10.1002/app.43071

INTRODUCTION

The manufacture of composites as new smart materials, materials which have one or more properties that can be significantly changed by external stimuli,[1–6] is a promising new area. In the pharmaceutical field, for instance, some of these composites are used as responsible drug delivery systems, improving the therapeutic efficacy of the treatments.[7–12] Nowadays, the science behind drug delivery has entered new research fields, which include the release of different active substances such as pesticides,[13,14] fertilizers,[15,16] nutrients,[17,18] and flavors.[19,20]

Deep marine carbonate rocks are key targets of offshore oil and gas exploration[21] since these rocks form significant hydrocarbon reservoirs.[22] As some of these rocks present an alkaline nature,[23] the drilling efficiency,[24] which is ordinarily measured as rate of penetration (ROP), decreases with the increase of the rocks' density.[25] Thus, ROP can be improved by the use of fracturing fluids[26] containing enzymes[27] or strong acids, such as hydrochloric acid, which is able to reduce the density of the carbonaceous formations.[28]

Thus, in this work, we present a proof-of-concept study for the application of a smart cardanol-furfural resin able to trap and release HCl from fracturing fluids. As far as we know, hydrochloric acid has never been trapped in this kind of polymer system. In addition, the resin was filled with alumina, a known abrasive particle,[29,30] and the obtained composites were coated with paraffin, producing a material able to respond to an external stimulus, in this case an increase in temperature. This increase in temperature acts as a trigger, allowing the controlled release of the strong acid contained into the composites. The materials produced were characterized by Fourier transform spectroscopy (FTIR), X-ray diffraction (XRD), thermal gravimetric analysis (TGA), differential scanning calorimetry (DSC), and scanning electron microscopy (SEM). In addition, measurements of pH as a function of the temperature were also performed. The results obtained are very encouraging because the

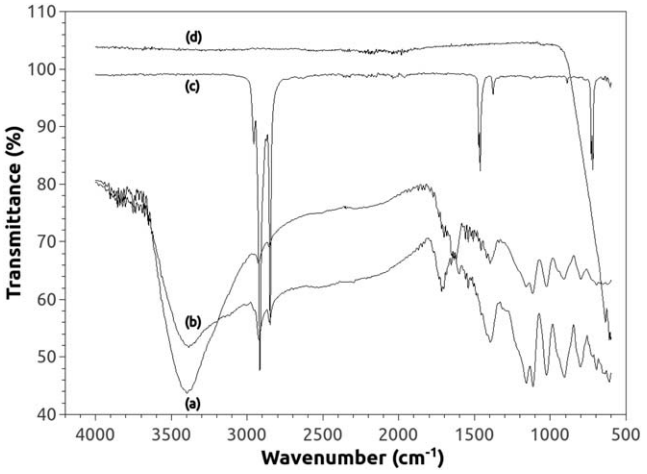

Figure 1. Spectra of (a) resin and composites containing composite filled with 15 wt % of alumina (b) without and (c) with the paraffin shell and (d) alumina.

materials produced are able to keep the pH of the water unchanged up to the start of the fusion of the paraffin. Therefore, these materials are potentially useful to the drilling industry.

EXPERIMENTAL

Materials

Alumina from Ascontec Abrasivos (Lorena-São Paulo, Brazil), solid paraffin (melting point equal to 57°C) from REDUC/PETROBRAS (Rio de Janeiro - Rio de Janeiro, Brazil), and cardanol from Resibras (Frtaleza-Ceará, Brazil) were kindly provided and used as received. Furfural and HCl, both analytical grade, were purchased from Vetec, Rio de Janeiro, Brazil. All reactants were used as received without further purification.

Polymerization and Preparation of the Composites

Cardanol and furfural resins were prepared through acid catalysis as described elsewhere.[31] In a general procedure, cardanol (25 g) and furfuraldehyde (17 g) were poured into a three-necked flask under continuous stirring at 70°C. Soon afterwards, the medium was acidified with hydrochloric acid (12*M*, 40 mL) and then stirred until a solid material formed. The composite materials were prepared using a similar experimental procedure. In this case, seeking to ensure the complete dispersion of the alumina in the reaction medium, the abrasive filler was inserted before acidification in three different amounts equal to 5, 10, and 15 wt % in the composites. Furthermore, composites were milled until they could pass through a 200-mesh sieve (~75 μm). The obtained particles were dispersed in 10 g of melted paraffin. Particles were removed from the medium using a nylon sieve and then were poured into a mortar, where the paraffin became solid. The particles were mechanically dispersed using a pestle.

Characterization

Fourier Transform Spectroscopy. The samples were analyzed by FTIR-ATR. FTIR analyses were performed on Nicolet iN10 equipment in which was coupled the attenuated total reflection (ATR) accessory (germanium crystal). The parameters used were a resolution of 4 cm^{-1} and an analyzed range between 4000 and 650 cm^{-1}.

X-ray Diffraction. The XRD experiments were performed on a Rigaku Miniflex diffractometer model, 2θ angle of 2° to 80°, the method FT (fixed time), in steps of 0.05° per second. The analysis was performed at room temperature with Cu Kα ($\lambda = 1.5418$ Å). This technique allows observation of the characteristic peak of alumina in the composites and pure alumina.

Scanning Electron Microscopy. Experiments were performed with a JEOL JSM-5610 LV microscope using an acceleration voltage of 15 kV. Samples were coated with gold in order to study the morphology of the prepared materials.

Thermogravimetric Analysis. TGA tests were performed using a Perkin-Elmer STA6000. Measurements were carried out using a sample mass around 25 mg, under nitrogen flow (20 mL/min), from 25°C to 700°C, at a heating rate of 20°C/min.

Differential Scanning Calorimetry. The thermal properties of paraffin were studied by DSC performed in the equipment TA Instruments DSC Q-1000 V9.9 Build 303. Measurements were carried out using a sample mass around 15 mg, under nitrogen flow (50 mL/min), from −80°C to 190°C, at a heating rate of 10°C/min.

Cure Degree. Cure degree was determined by the extraction method,[32] using toluene as solvent. Materials were kept inside the Soxhlet extractor for 48 h. The percentage of crosslinked material (%R) was calculated using eq. (1):

$$(\%R) = (W/W_o) \times 100 \quad (1)$$

where W is the sample weight after drying and W_o is the initial weight of the sample before extraction.

Acid Released from the Paraffin-Coated Composites. For each test, one gram of composite was studied using the USP

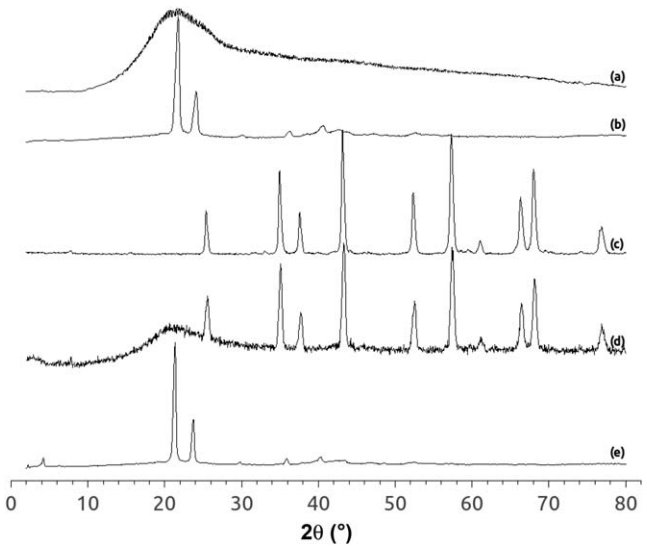

Figure 2. XRD patterns of (a) resin, (b) paraffin, (c) alumina, and composite filled with 15 wt % of alumina (d) without and (e) with the paraffin shell.

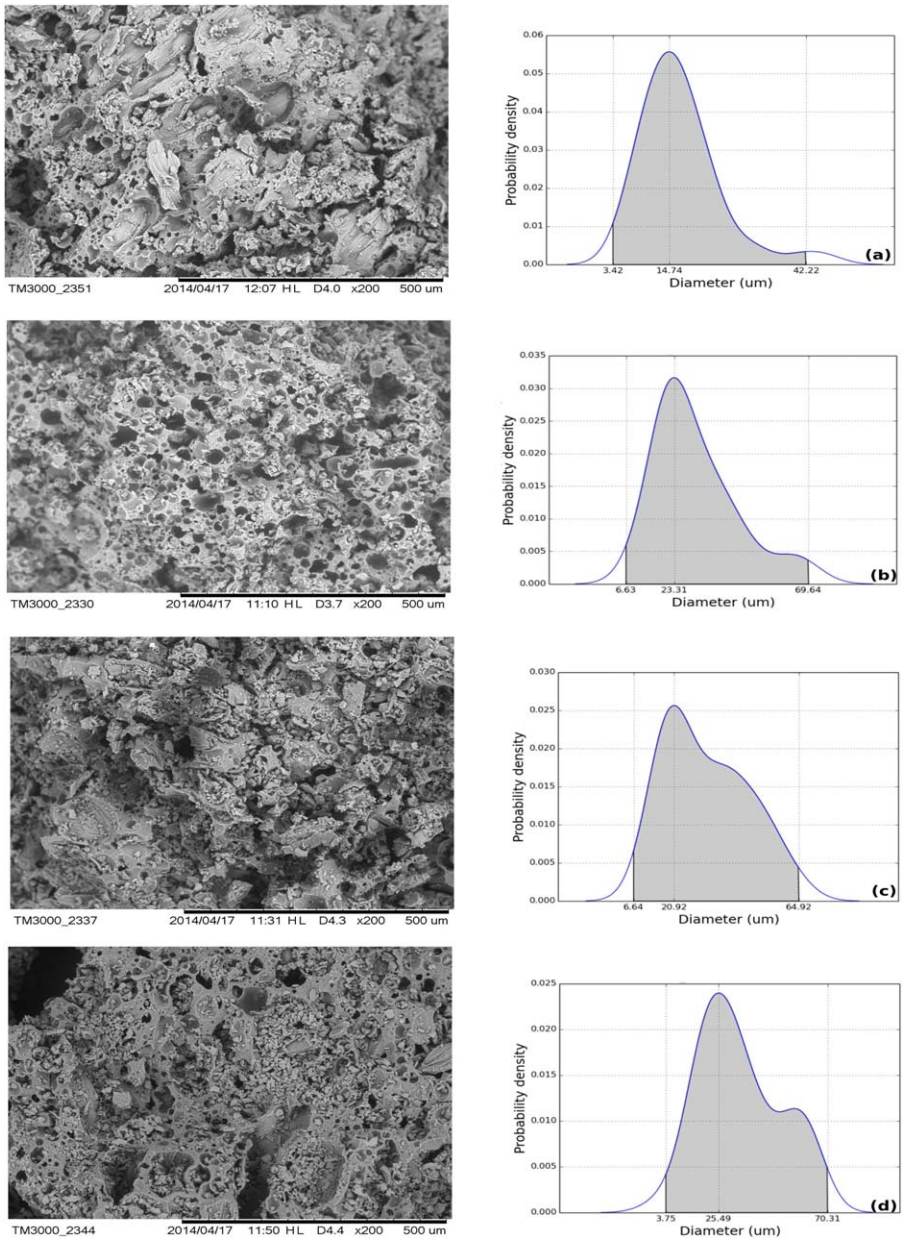

Figure 3. SEMs and respective PDFs of (a) bioresin, composites filled using (b) 5 wt %, (c) 10 wt %, and (d) 15 wt % of alumina. [Color figure can be viewed in the online issue, which is available at wileyonlinelibrary.com.]

Apparatus I at 75 rpm. The released amount of acid was analyzed in distilled water (1 L). Temperature was increased using a heating rate equal to 5°C/min, and samples were collected at 23, 28, 38, 48, 57, and 67°C. All of these tests were performed in triplicate. A pH meter (Novatecnica model NTPHM) was used to determine the acidity of the solution.

RESULTS AND DISCUSSION

The composites showed a high degree of cure, which was, on average, equal to $(85 \pm 7)\%$. This high degree of cure helps to ensure the complete immobilization of alumina particles inside the organic matrix, producing a thermoset and abrasive material.

Figure 1 shows the FTIR spectra of the tested materials. Figure 1(a) shows the spectrum of the resin, which presents a wide band at 3342 cm^{-1} related to OH stretching. This band is wide because the OH group presents a high capability to form hydrogen bonds. There is a decrease in the intensity of this band in the bioresin spectrum compared with the cardanol one. This intensity decrease means that the polymerization took place through the phenolic group preserving the aliphatic chain. The presence of a characteristic band around 1640 cm^{-1}, associated with the C=C axial deformation, corroborates this information. The doublet observed at 2921 and 2846 cm^{-1} corresponds to CH_2 and CH_3 stretching. The low intensity of this doublet can be associated with the high degree of crosslinking.[33] Figure 1 also shows the spectra of the composite filled with 15 wt % of

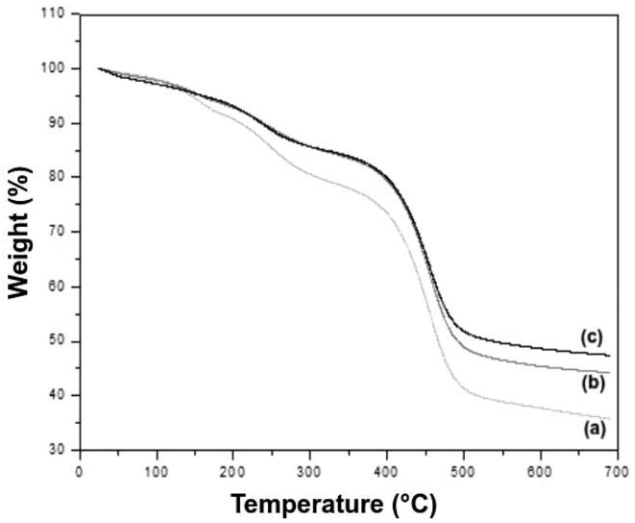

Figure 4. TGA curves of the composites filled with (a) 5 wt %, (b) 10 wt %, and (c) 15 wt % of alumina without paraffin.

alumina before [Figure 1(b)] and after [Figure 1(c)] the use of paraffin as a shell. The FTIR of the composite without paraffin is quite similar to the one of the pure resin, presenting most of its characteristic bands. In turn, FTIR of the paraffin-coated composite is identical to the one of the pure paraffin. This last presents a doublet at 2915 cm^{-1} and 2846 cm^{-1}, related to CH_3 and CH_2 axial deformation. The characteristic peak at 1459 cm^{-1} is associated with the CH_2 and CH_3 symmetric angular deformation, and the characteristic peak at 719 cm^{-1} corresponds to the CH_2 and CH_3 asymmetric angular deformation in alkanes.[33] This is a very promising result because FTIR-ATR is a surface analysis,[34] which indicates the success of the coating process. Finally, alumina [Figure 1(d)] presents a single characteristic band around 575 cm^{-1}, which is assigned to Al—O vibrations.[35]

Figure 2 shows the XRD patterns of the resin, paraffin, alumina, and composite filled with 15 wt % of alumina before and after the use of paraffin as a shell. Resin is amorphous. Alumina presents diffraction peaks centered at 2θ equal to 25.4°, 34.9°, 37.6°, 43.2°, 52.3°, 57.4°, 61.1°, 66.4°, 68.0°, and 76.9°. These results are in complete agreement with the literature.[36] In turn, the composite filled with 15 wt % of alumina presents an amorphous halo, from resin, centered at 21.3°, besides the crystalline peaks related to the alumina phase, centered at 2θ equal to 25.7°, 35.1°, 37.8°, 43.3°, 52.5°, 57.5°, 61.2°, 66.5°, 68.2°, and 76.9°. These results lead to the conclusion that, as expected, the preparation process of the composites did not change the structure of the alumina, thus preserving its properties as an abrasive particle, allowing the use of the composites in drilling applications. Figure 2 also shows the XRD pattern of the paraffin, which presents diffraction peaks centered at 2θ equal to 21.8°, 24.1°, 30.0°, 36.3°, and 40.6°. These results are also in complete agreement with the literature.[37,38] In turn, the paraffin-coated composite, as discussed in the FTIR analysis, presents only the paraffin peaks, in this case centered at 2θ equal to 21.4°, 23.7°, 29.7°, 35.9°, and 40.4°. Therefore, this result is in complete agreement with the FTIR one, proving that the coating process of the composites with paraffin was efficient.

The scanning electron micrograph of the bioresin and composites filled with 5 wt %, 10 wt %, and 15 wt % of alumina without paraffin, as well as the probability distribution functions (PDF) of their observed micropores, are shown in Figure 3. As one can see, all of the tested materials presented multiple micropores. These micropores are due to the presence of hydrochloric acid, which promotes the formation of voids where this active substance remains trapped. The diameter distribution of these pores was also studied. The PDFs shown in Figure 3 are useful to describe the spread of experimental data around a sample average and can be interpreted as a smoothed histogram. The commonest PDF is the normal distribution,[39,40] which, as described by Bard,[41] is very useful because of its simplicity. However, as in the present case, experimental fluctuations can follow rather different distribution functions, which can be used for interpretation of the experimental technique and of the experimental data. Therefore, PDF analysis shows that the spread of pore data is more complex, so, using a non-Gaussian representation, the diameter of pores of the bioresin and composites filled with 5 wt %, 10 wt %, and 15 wt % of alumina are equal to 15^{+27}_{-11}, 23^{+43}_{-17} , 21^{+44}_{-14} , and 25^{+45}_{-22} μm, respectively. These diameters correspond to volumes equal to $1.68^{+0.40}_{-1.66} \times 10^{-9}$, $4.79^{+0.01}_{-4.67} \times 10^{-9}$, $8.67^{+0.02}_{-8.65} \times 10^{-9}$, and $6.63^{+0.02}_{-6.48} \times 10^{-9}$ mL, respectively. Therefore, as the calculated volumes are statistically equal, the tested samples possess statistically the same capability to trap the active substance, and the presence of alumina does not affect it.

Figure 4 shows the TGA of the composites without paraffin. There are three main mass loss events. The first, around 110°C, and the second, around 210°C, are associated with the elimination of hydrochloric acid[42] and low molecular weight volatiles, respectively. This is an important result, which allows us to

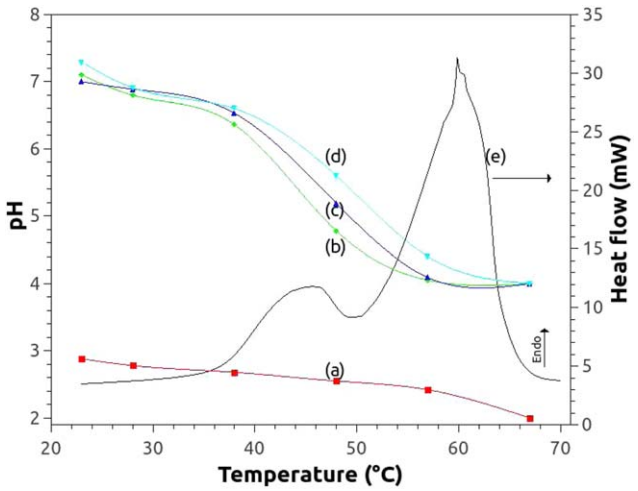

Figure 5. (a) Acid released from composite filled with 15 wt % of alumina without paraffin shell; paraffin-coated composites and filled with (b) 5 wt %, (c) 10 wt %, and (d) 15 wt % of alumina; and (e) DSC thermogram of the pure paraffin. [Color figure can be viewed in the online issue, which is available at wileyonlinelibrary.com.]

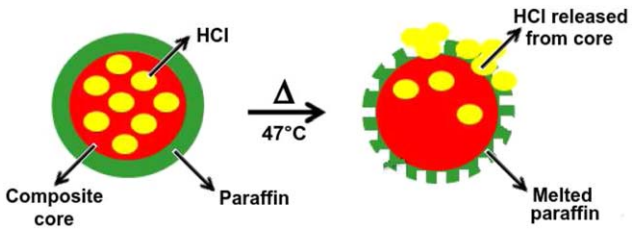

Figure 6. Changes in the composite structure triggered by an external stimulus leading to the release of the trapped acid. [Color figure can be viewed in the online issue, which is available at wileyonlinelibrary.com.]

conclude that HCl is trapped inside the composites under 100°C. In turn, the third one, around 390°C, is related to the thermal decomposition of the polymer.[43] Figure 5 also shows that the increase of the used amount of alumina produces an increase of the residue amount, besides improving the thermal stability of the materials. Therefore, materials filled with 5 wt %, 10 wt %, and 15 wt % of alumina were thermally stable up to 381°C, 409°C, and 411°C, respectively. The same samples presented residues at 650°C equal to 36.7 wt %, 43.2 wt %, and 46.4 wt %, respectively.

The acid release test of the composites is shown in Figure 5. The results imply that the coating process with the paraffin was similar to all composites and the amount of paraffin used was enough to keep the acidity levels at room temperature, ensuring that the acid is just released from the onset of melting of the paraffin. This is confirmed on the same graph by examining the results of the paraffin melting test, performed using the DSC. This test showed that the beginning of the paraffin melting process occurred around 34°C. From this temperature, the acidity of the medium increases, reaching its maximum value when all of the paraffin melts at 60°C. This phenomenon can be exemplified using the mechanism proposed in Figure 6. According to the proposed model, acid is trapped inside the composites, remaining inactive in the structure while the melting temperature of the paraffin shell is not reached. After this, acid is released and the pH decreases, as shown in Figure 5.

Thus, the experiments performed show that the release of active systems can be engineered to act under specific conditions, as expected in smart composites.

CONCLUSIONS

The preparation of green and abrasive composites in the presence of a strong acid was performed. The paraffin-coated materials obtained presented an interesting acid-release profile that is triggered by temperature. As soon as the paraffin melts, the smart composite starts to release its trapped acid, producing an increase of the H^+ concentration, which became around 800 times larger than the initial one. This increase of the acid concentration is able to produce the reaction between the $CaCO_3$ present in sedimentary rocks with the HCl released from the composite, allowing us to conclude that drilling operations can be faster in the presence of this smart composite.

ACKNOWLEDGMENTS

The authors thank Conselho Nacional de Desenvolvimento Científico e Tecnológico (CNPq-474940/2012-8 and BN 550030/2013-1), Coordenação de Aperfeiçoamento de Pessoal de Nível Superior (CAPES and CAPES-MES Cuba 154/12), Financiadora de Estudos e Projetos (FINEP PRESAL Ref. 1889/10), FAPERJ (Brazil http://dx.doi.org/10.13039/501100004586) the LABEST/PEC/COPPE/UFRJ laboratory for SEM, Ascontec Abrasivos for alumina powder, Reduc/Petrobras for paraffin, and Fundação Carlos Chagas Filho de Amparo à Pesquisa do Estado do Rio de Janeiro (FAPERJ) for the financial support and scholarships.

REFERENCES

1. Maiti, D. K.; Sinha, P. K. *Procedia Eng.* **2011**, *14*, 3268.
2. Song, Y.; Kim, S.; Park, I.; Lee, U. *Thin-Walled Struct.* **2015**, *89*, 84.
3. Shabana, Y. M.; Ristinmaa, M. *Int. J. Solids Struct.* **2011**, *48*, 3209.
4. Pérez, R. A.; Won, J.-E.; Knowles, J. C.; Kim, H.-W. *Adv. Drug Delivery Rev.* **2013**, *65*, 471.
5. Payandeh, Y.; Meraghni, F.; Patoor, E.; Eberhardt, A. *Mater. Des.* **2012**, *39*, 104.
6. Roh, J.-H.; Kim, J.-S.; Kwon, O.-H. *Compos. Struct.* **2015**, *125*, 417.
7. Pereira, E. D.; Souza, Jr., F. G.; Pinto, J. C. C. S.; Cerruti, R.; Santana, C. *Macromol. Symp.* **2014**, *343*, 18.
8. Pereira, E. D.; Souza, F. G.; Santana, C. I.; Soares, D. Q.; Lemos, A. S.; Menezes, L. R. *Polym. Eng. Sci.* **2013**, *53*, 2308.
9. Krawczak, P. *eXPRESS Polym. Lett.* **2013**, *7*, 651.
10. Nkabinde, L. A. *eXPRESS Polym. Lett.* **2013**, *8*, 197.
11. Ke, Y. *eXPRESS Polym. Lett.* **2014**, *8*, 841.
12. Hamad, K. *eXPRESS Polym. Lett.* **2015**, *9*.
13. Singh, B.; Sharma, D. K.; Kumar, R.; Gupta, A. *J. Hazard. Mater.* **2010**, *177*, 290.
14. Van Woerkom, A. H.; Aćimović, S. G.; Sundin, G. W.; Cregg, B. M.; Mota-Sanchez, D.; Vandervoort, C.; Wise, J. C. *Crop Prot.* **2014**, *65*, 173.
15. Santos, B. R. dos; Bacalhau, F. B.; Pereira, T. dos, S.; Souza, C. F.; Faez, R. *Carbohydr. Polym.* **2015**, *127*, 340.
16. Yardin, M. R.; Kennedy, I. R.; Thies, J. E. *Radiat. Phys. Chem.* **2000**, *57*, 565.
17. Gao, Q.; He, Y.; Fu, J.; Liu, A.; Ma, L. *Biomater.* **2015**, *61*, 203.
18. Harris, N. B.; Tucker, G. E. *Sediment. Geol.* **2015**, *323*, 31.
19. Ziani, K.; Fang, Y.; McClements, D. *J. Food Res. Int.* **2012**, *46*, 209.
20. Belingheri, C.; Ferrillo, A.; Vittadini, E. *LWT - Food Sci. Technol.* **2015**, *60*, 593.
21. Wenzhi, Z.; Suyun, H.; Wei, L.; Tongshan, W.; Yongxin, L. *Nat. Gas Ind. B* **2014**, *1*, 14.
22. van der Land, C.; Wood, R.; Wu, K.; van Dijke, M. I. J.; Jiang, Z.; Corbett, P. W. M.; Couples, G. *Mar. Pet. Geol.* **2013**, *48*, 1.

23. Ulbrich, H. H. G. J.; Gomes, C. B. *Earth Sci. Rev.* **1981**, *17*, 135.
24. Lopes, G.; de Oliveira, T. C.; do, C.; Pérez-Gramatges, A.; da Silva, J. F. M.; Nascimento, R. S. V. *J. Appl. Polym. Sci.* **2014**, *131*, n/a.
25. Company, R. M. In Handbook of Ground Water Development; John Wiley & Sons: New York, USA, **1990**, p 512.
26. Barati, R.; Liang, J.-T. *J. Appl. Polym. Sci.* **2014**, *131*, n/a.
27. Barati, R.; Johnson, S. J.; McCool, S.; Green, D. W.; Willhite, G. P.; Liang, J.-T. *J. Appl. Polym. Sci.* **2011**, *121*, 1292.
28. Huitt, J. L. **1969**. Method of Fracturing and Enlarging the Fracture with Acid. US Patent 3455388, http://www.freepatentsonline.com/3455388.html, Accessed October 7, 2015.
29. Khumalo, V. M. *eXPRESS Polym. Lett.* **2010**, *4*, 264.
30. Poostforush, M. *eXPRESS Polym. Lett.* **2013**, *8*, 293.
31. Varela, A.; Oliveira, G.; Souza, F. G.; Rodrigues, C. H. M.; Costa, M. A. S. *Polym. Eng. Sci.* **2013**, *53*, 44.
32. Forrest, M. J. In Analysis of Thermoset Materials, Precursors and Products; iSmithers Rapra Publishing: Shropshire, UK, **2003**, p 164.
33. Silverstein, R. M.; Webster, F. X.; Kiemle, D. J. In Spectrometric Identification of Organic Compounds; John Wiley & Sons: New York, USA, **2005**, p 522.
34. Planinsek, O.; Planinsek, D.; Zega, A.; Breznik, M.; Srcic, S. *Int. J. Pharm.* **2006**, *319*, 13.
35. Khoshkhan, Z.; Salehi, M. J. *Nanostruct.* **2014**, *4*, 443.
36. Feret, F. R.; Roy, D.; Boulanger, C. *Spectrochim. Acta, Part B* **2000**, *55*, 1051.
37. Zhang, Z.; Zhang, N.; Peng, J.; Fang, X.; Gao, X.; Fang, Y. *Appl. Energy* **2012**, *91*, 426.
38. Yunfeng, T.; Yang, W.; Ping, Z.; Lingyi, J. *Chinese J. Mater. Res.* **2015**, *29*, 262.
39. Souza, Jr., F. G.; Pinto, J. C.; Soares, B. G. *Eur. Polym. J.* **2007**, *43*, 2007.
40. de Souza, Jr., F. G.; Soares, B. G.; Pinto, J. C. *Eur. Polym. J.* **2008**, *44*, 3908.
41. Bard, Y. In Nonlinear Parameter Estimation; Academic Press: Minnesota, USA, **1974**, p 356.
42. Vogel, A. I. In Vogel's Textbook of Quantitative Chemical Analysis; Prentice Hall: London, UK, **2000**, p 844.
43. Manjula, S.; Pillai, C. K. S.; Kumar, V. G. *Thermochim. Acta* **1990**, *159*, 255.